Cumulene Structures

DOI: 10.1002/ange.201310975

C_4 Cumulene and the Corresponding Air-Stable Radical Cation and Dication**

Yan Li, Kartik Chandra Mondal, Prinson P. Samuel, Hongping Zhu, Claudia M. Orben, Saravanan Panneerselvam, Birger Dittrich,* Brigitte Schwederski, Wolfgang Kaim,* Totan Mondal, Debasis Koley,* and Herbert W. Roesky**

Dedicated to Professor Hubert Schmidbaur on the occasion of his 80th birthday

Abstract: *A neutral C_4 cumulene **1** that includes a cyclic alkyl(amino) carbene (cAAC), its air-stable radical cation $\mathbf{1}^{\bullet+}$, and dication $\mathbf{1}^{2+}$ have been synthesized. The redox property of $\mathbf{1}^{\bullet+}$ was studied by cyclic voltammetry. EPR and theoretical calculations show that the unpaired electron in $\mathbf{1}^{\bullet+}$ is mainly delocalized over the central C_4 backbone. The commercially available CBr_4 is utilized as a source of dicarbon in the cumulene synthesis.*

Recent research on species with low-valent elements and main-group radicals has achieved tremendous success by employing an N-heterocyclic carbene (NHC) as a ligand.[1] cAAC[2] is one of the stable carbenes, which is shown by theoretical calculations to have a singlet spin ground state with a smaller HOMO–LUMO energy gap when compared with NHCs.[1b,2b,c] Moreover, recent studies on cAAC show that this molecule is more nucleophilic and also more electrophilic than NHCs.[2d] This significantly influences the chemical property of the products. Radicals centered on main-group elements, such as $PN^{\bullet+}$,[3] $P_2^{\bullet+}$,[4] phosphinyl radical cations,[5] $H\text{-}B^{\bullet+}$,[6] and ketenes with biradical character,[7] can be successfully stabilized and isolated by utilizing cAAC. Previously, we reported the syntheses of novel acyclic silylone $(cAAC)_2Si$[8] and germylone $(cAAC)_2Ge$.[9] These compounds are the congeners of allenes, which exhibit biradicaloid character. Furthermore, a $(cAAC)_2(Si_2Cl_2)$ compound was prepared as a silicon analogue of 1,3-butadiene.[10] Although cAAC-stabilized silicon and germanium adducts were successfully synthesized, the related chemistry of carbon has not yet been reported.

Carbene-stabilized carbon(0) species, which possess a ylidone structure (C:→:C:←:C), have been experimentally prepared and theoretically analyzed by Bertrand and Frenking et al.[11] However, the synthesis of analogous $(carbene)_2C_2$ has not been achieved, although compounds $(NHC)_2Si_2$[1a] and $(NHC)_2Ge_2$[12] with the sister elements of carbon were documented. Very recently, a Lewis base stabilized dicarbon (C_2) system has been theoretically predicted,[13] which is considered as a terminally functionalized 1,1,4,4-tetraamino C_4-cumulene.[14] The general methods for synthesizing a C_4 unit include metal-mediated C–C coupling of two smaller precursors (C_n and C_{4-n}) or functional transformation of a preformed C_4 unit.[14a] Cumulene carbon chains show redox activity when they are connected terminally with transition metals.[15] However, their radical species were only detected spectroscopically as unexpected intermediates.[16] On the basis of the known carbene chemistry, we were curious to introduce cAAC as a precursor into the synthesis of a cumulene. Herein, we present the isolation of such

[*] Y. Li, Prof. Dr. H. Zhu
State Key Laboratory of Physical Chemistry of Solid Surfaces
College of Chemistry and Chemical Engineering, Xiamen University
Xiamen, Fujian, 361005 (China)
E-mail: hpzhu@xmu.edu.cn
Dr. K. C. Mondal, Dr. P. P. Samuel, C. M. Orben, Prof. Dr. H. W. Roesky
Institut für Anorganische Chemie
Georg-August-Universität
Tammannstrasse 4, 37077 Göttingen (Germany)
E-mail: hroesky@gwdg.de
Dr. S. Panneerselvam
Deutsches Elektronen-Synchrotron
Notke Strasse 85, 22607 Hamburg (Germany)
Priv.-Doz. Dr. B. Dittrich
Universität Hamburg
Martin-Luther-King-Platz 6, 20146-Hamburg (Germany)
E-mail: birger.dittrich@chemie.uni-hamburg.de
T. Mondal, Dr. D. Koley
Department of Chemical Sciences
Indian Institute of Science Education and Research (IISER)
Kolkata Mohanpur Campus, Mohanpur 741252 (India)
E-mail: koley@iiserkol.ac.in
Dr. B. Schwederski, Prof. Dr. W. Kaim
Universität Stuttgart, Institut für Anorganische Chemie
Pfaffenwaldring 55, 70569 Stuttgart (Germany)
E-mail: kaim@iac.uni-stuttgart.de

[**] H.W.R. acknowledges the Deutsche Forschungsgemeinschaft for financial support (RO 224/60-1). T.M. is thankful to CSIR for the JRF fellowship. D.K. acknowledges IISER-Kolkata for start-up grant and SERB for DST fast track fellowship (SR/FT/CS-72/2011). B.D. acknowledges I. Nevoigt (Universität Hamburg) for the assistance of data collection. Y.L. thanks China Scholarship Council (CSC/91027014) for a fellowship. A part of this work was carried out at the PetraIII light source at DESY, a member of the Helmholtz Association (HGF).

Supporting information for this article is available on the WWW under http://dx.doi.org/10.1002/anie.201310975.

a cumulene-type dicarbon (C_2) species and its redox chemistry.

In an initial experiment, THF was added to a mixture of cAAC (mixed with LiOTf salt),[2a] CBr_4, and K or Li in a molar ratio of 2:2:9 at room temperature, immediately forming a red suspension.[17] After vigorously stirring for 48 h, the suspension turned to brown and compound **1** was obtained as yellow crystals from the toluene extract (Scheme 1). Compound **1** is stable in air, even at high temperature. Therefore, a modified method of purification of **1** was developed. The reaction solution was dried and **1** was obtained in 52% yield by sublimation at 240°C (0.1 mmHg).

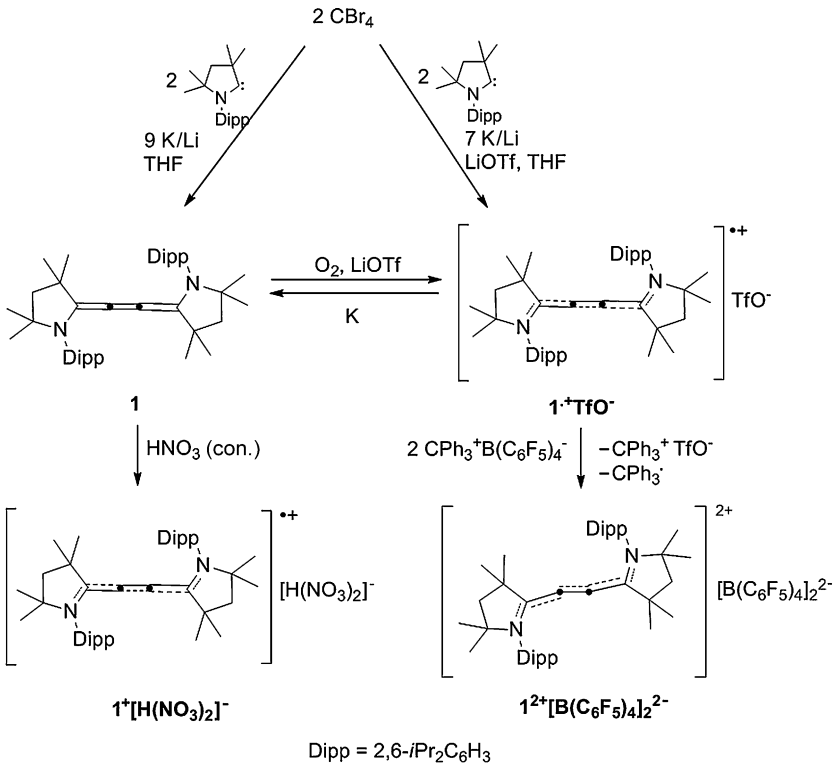

Scheme 1. Synthesis of cumulene **1** and its conversion into a radical cation and two dications.

Further exploration of an alternative reducing agent (KC_8) failed, and the formation of black carbon powder was observed. ^{1}H and ^{13}C NMR spectra of **1** clearly exhibit symmetric patterns, showing that both the cAAC units in **1** are equivalent. In the ^{13}C NMR spectrum of **1**, the resonance ($\delta = 176.2$ ppm) of the carbene carbons is shifted remarkably upfield when compared with that of cAAC ($\delta =$ 304.2 ppm).[2a] The related resonance of the central C_2 is shown at a higher field ($\delta = 71.2$ ppm). When a similar reaction was carried out utilizing NHC as a carbene source, the analogue of **1** was not obtained. To the best of our knowledge, synthesis of a cumulene employing any carbene has not yet been reported.

Surprisingly, after the separation of **1**, a red crystalline solid was slowly formed as part of the insoluble material, which was filtered and exposed to air along with a small amount of solvent. The X-ray diffraction analysis showed its **1**$^{\bullet+}$TfO$^-$ structure containing a C_4 cumulene radical cation and a TfO$^-$ counterion (see the Supporting Information). To confirm this transformation, a mixture of **1** and LiOTf (1:1.2) was stirred overnight in CH_2Cl_2 under exposure to air, and **1**$^{\bullet+}$TfO$^-$ was produced in high yield (Scheme 1). An alternative route to **1**$^{\bullet+}$TfO$^-$ was also developed. The reaction of cAAC (mixed with LiOTf salt), CBr_4, and K or Li in a molar ratio of 2:2:7 in THF smoothly led to **1**$^{\bullet+}$TfO$^-$ in 87% yield (Scheme 1). A plausible intermediate of this reaction is cAAC=C(Br)−C$^{\bullet}$=cAAC, which undergoes Li^+-triggered ionization via $Br^- \rightarrow TfO^-$ exchange. We envisage that **1** is the reductive product of **1**$^{\bullet+}$TfO$^-$ and both are stepwise formed by debromination of CBr_4. As expected, reduction of **1**$^{\bullet+}$TfO$^-$ with K exclusively afforded **1**, which was confirmed by NMR analysis. **1**$^{\bullet+}$TfO$^-$ is insoluble in toluene and *n*-hexane, but well-soluble in THF, CH_3CN, and CH_2Cl_2, indicating its ionic character. It is thermodynamically stable and has a clear melting point (205°C). Species **1**$^{\bullet+}$TfO$^-$ is NMR-silent, illustrating its paramagnetic nature. Owing to the insufficient crystallinity of **1**$^{\bullet+}$TfO$^-$, the quality of the crystal data is limited. However, an X-ray quality crystal of **1**$^{\bullet+}$TfO$^-$·THF·H_2O was obtained under slow evaporation of the THF solution of **1**$^{\bullet+}$TfO$^-$; the corresponding structure is shown in Figure 1.[18]

Compound **1** was characterized by X-ray crystallography (Figure 2). The C_4 backbone is centrosymmetric and almost linear. Both the carbene carbon atoms adopt a perfect planar geometry. The C1−C21 (1.3236(16) Å) and C21−C21i (1.249(2) Å) bond lengths, and the C1−C21−C21i angle (178.82(15)°) are comparable to those found in the reported cumulenes and the calculated case.[14a,13] In comparison to **1**, the bond lengths of **1**$^{\bullet+}$TfO$^-$·THF·H_2O change, which is due to the one-electron oxidation. The C1−C21 bond (1.373(4) Å) in **1**$^{\bullet+}$TfO$^-$·THF·H_2O is slightly elongated, while the C21−C21i bond (1.229(5) Å) is correspondingly shortened. Moreover, the endocyclic C1−N1 bond (1.338(5) Å) in **1**$^{\bullet+}$TfO$^-$·THF·H_2O is shortened by about 0.04 Å when compared with that in **1** (1.3817(17) Å), indicating the strengthening of the C−N bond that is due to the electron deficiency of the C_4 backbone.

The UV/Vis spectrum of **1** recorded in CH_2Cl_2 shows a weak absorption band at 535 nm, which is quite different from that of **1**$^{\bullet+}$TfO$^-$ (535(s), 495, 466, 408(s), 388 nm).

The EPR spectrum of **1**$^{\bullet+}$TfO$^-$ was recorded in THF solution at room temperature, centered at $g = 2.0032$. The relatively small ^{14}N hyperfine coupling of 5.3 Gauss (quintet 1:2:3:2:1 for two equivalent nitrogen atoms, Figure 3) reflects the concentration of spin on the C_4 backbone with limited participation of the nitrogen centers. This is in agreement with

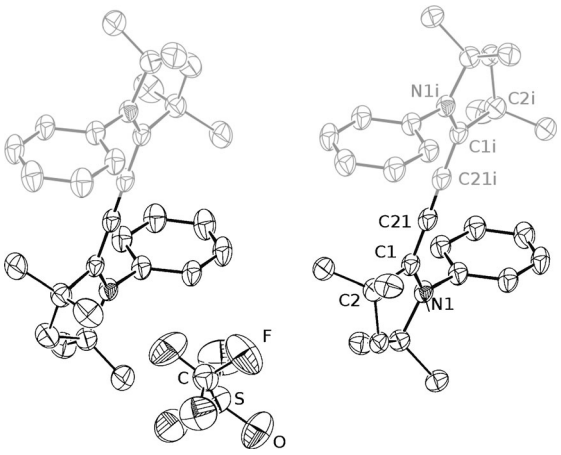

Figure 1. Molecular structure of $\mathbf{1}^{\bullet+}TfO^{-}\cdot THF\cdot H_2O$. Ellipsoids are set at 50% probability; hydrogen atoms, *i*Pr groups, and solvent molecules are omitted for clarity. The second halves of the C_4 units symmetrically generated are displayed in gray. Only one TfO^- is shown. Owing to the essential similarity between the two C_4 units, selected bond lengths (Å) and angles (°) of one labeled C_4 unit are given (calculated values at the M06-2X/SVP level of theory are listed in square brackets): N1–C1 1.338(5)[1.333], C1–C21 1.373(4)[1.375], C21–C21i 1.229(5)[1.240]; N1-C1-C2 112.08(21)[111.91], C21-C1-N1 123.18(21)[123.13], C21-C1-C2 124.74(24)[124.95], C21i-C21-C1 176.38(26)[178.68].

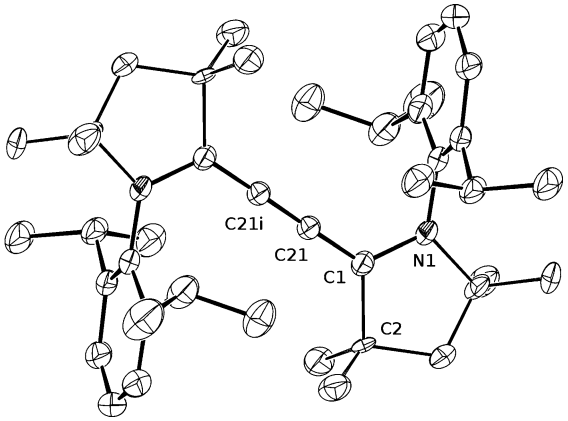

Figure 2. Molecular structure of **1.** Ellipsoids are set at 50% probability; hydrogen atoms and solvent molecule (toluene) are omitted for clarity. Selected bond lengths (Å) and angles (°) (calculated values at the M06-2X/SVP level of theory are listed in square brackets): N1–C1 1.3817(17)[1.387], C1–C21 1.3236(16)[1.333], C21–C21i 1.249(2)-[1.272]; N1-C1-C2 108.74(28)[109.35], C21-C1-N1 123.87(10)[124.48], C21-C1-C2 127.37(25)[126.14], C21i-C21-C1 178.86(14)[178.80].

structural and computational results (see the Supporting Information). Radical ions of 1,2,3-butatriene were reported but they were only characterized by EPR spectroscopy.[16] The coupling of ^1H with remote substituents is expectedly small and may only contribute to the overall linewidth of two Gauss peak-to-peak difference. The ^{13}C hyperfine interactions could not be observed as satellites of the main lines and must be smaller than 8 Gauss, in agreement with the DFT calculation.

Compound $\mathbf{1}^{\bullet+}TfO^-$ is redox-active and exhibits one reversible one-electron reduction at $E_{1/2} = -0.313$ V versus Fc^+/Fc in the cyclic voltammogram, which corresponds to

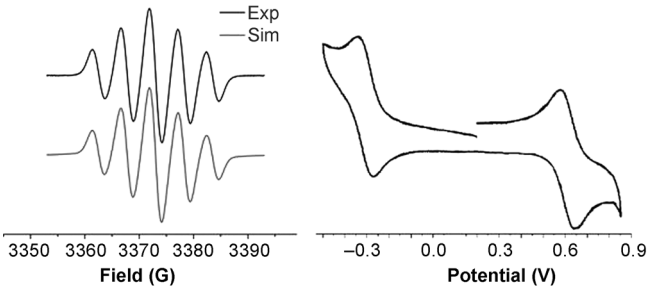

Figure 3. Left: X-band EPR spectrum recorded in THF solution at room temperature for $\mathbf{1}^{\bullet+}TfO^-$. ($g = 2.0032$); Right: Cyclic voltammogram for a CH_3CN solution of $\mathbf{1}^{\bullet+}TfO^-$, containing 0.1 M $n Bu_4NPF_6$ as electrolyte (potential versus Fc^+/Fc, scan rate 100 $mV s^{-1}$).

$\mathbf{1}^{\bullet+} \rightarrow \mathbf{1}$ (Figure 3). Interestingly, another reversible one-electron oxidation is shown at $E_{1/2} = 0.608$ V, prompting us to further explore the potential of a dication by employing stronger oxidizing agents.

As anticipated, treatment of **1** with concentrated HNO_3 successfully produced $\mathbf{1}^{2+}[H(NO_3)_2^-]_2$ as yellow crystals (Scheme 1). An alternative way by the oxidation of $\mathbf{1}^{\bullet+}TfO^-$ with $CPh_3^+B(C_6F_5)_4^-$ in CH_2Cl_2 also produced the brown-red dication $\mathbf{1}^{2+}[B(C_6F_5)_4^-]_2$ (see Scheme 1 and the Supporting Information). Both compounds are hardly soluble in organic solvents and show high melting points (296 and 302 °C, respectively). The molecular structure of $\mathbf{1}^{2+}[H(NO_3)_2^-]_2$ is shown in Figure 4.[19] On the one hand, the C1–C21 bond (1.4367(10) Å) in $\mathbf{1}^{2+}[H(NO_3)_2^-]_2$ is longer than those in **1** and $\mathbf{1}^{\bullet+}$. On the other hand, the C21–C21i bond (1.1855(14) Å) is greatly shortened, which falls in the range of a triple bond. Moreover, the endocyclic C1–N1 bond distance (1.2865(9) Å) in $\mathbf{1}^{2+}[H(NO_3)_2^-]_2$ is significantly shorter, by about 0.05 and 0.1 Å, than those in **1** and $\mathbf{1}^{\bullet+}$, respectively. This change indicates the C–N double-bond character that is due to the increase of electron deficiency of the C_4 backbone.

For a better understanding of the structural, electronic, and redox properties, geometry optimization of **1** was per-

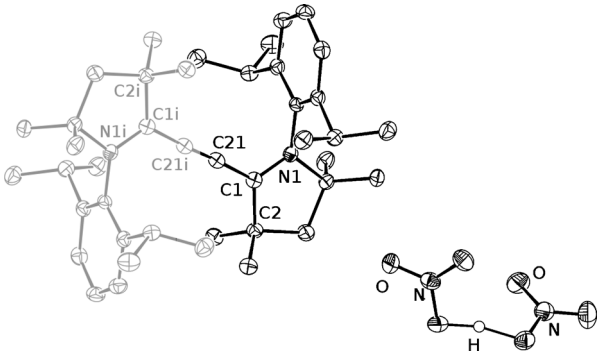

Figure 4. Molecular structure of $\mathbf{1}^{2+}[H(NO_3)_2^-]_2$. Ellipsoids are set at 50% probability; hydrogen atoms in the C_4 unit are omitted for clarity. The second half of the C_4 unit which is symmetrically generated is displayed in gray. Only one $H(NO_3)_2^-$ is shown. Selected bond lengths (Å) and angles (°) (calculated values at the M06-2X/SVP level of theory are listed in square brackets): N1–C1 1.2865(9)[1.288], C1–C21 1.4367(10)[1.431], C21–C21i 1.1855(14)[1.211]; N1-C1-C2 115.37(7)-[114.61], C21-C1-N1 120.41(7)[121.48], C21-C1-C2 124.22(7)[123.90], C21i-C21-C1 177.58(11)[176.82].

formed at the M06-2X/SVP level of theory.[20] Optimizations at both the singlet and triplet states reveal the singlet state to be the electronic ground state with an energy difference (ΔE_{ST}) of 31.2 kcal mol^{-1}. The energy-minimized structures show strong resemblance with the X-ray crystal structure as seen from the alignments and superposition of the respective geometries (Supporting Information, Figure S9).

The HOMO and HOMO−3 of **1** show strong π-interactions along C21−C21i and C1−C21/C21i−C1i bonds with additional electron densities localized on the nitrogen lone pairs (Figure 5a). A similar electron density distribution was reported by Dutton and Wilson in the DFT study of NHC-

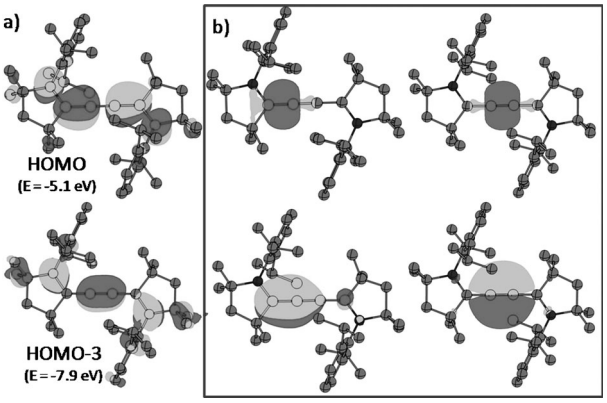

Figure 5. a) KS-HOMO and KS-HOMO−3 of **1**; b) Selected NLMOs of **1**. The orbital energies (*E*) are shown in brackets.

stabilized C_2 analogues.[13a] Selected natural localized molecular orbitals (NLMOs) of the C21−C21i bond (at M06-2X/TZVP//M06-2X/SVP level) are plotted to emphasize the bonding environment along the C1−C21−C21i−C1i (C_4) backbone (Figure 5b). The calculated Wiberg bond indices (WBI), at M06-2X/TZVP//M06-2X/SVP level, of C21−C21i and C1−C21/C21i−C1i bonds are 2.07 and 1.62 Å, respectively (Supporting Information, Table S2). The values indicate that both the central C_2 core and the terminal bonds possess double bond character; the former is to a greater extent. Removal of an electron from the HOMO (Figure 5a) results in the depletion of electron density on the terminal C1−C21/C21i−C1i bonds. This understanding is in agreement with the fact that oxidation of **1** to a radical cation ($\mathbf{1}^{\bullet+}$) results in the elongation of C1−C21/C21i−C1i bond along with the shortening of C21−C21i and N1−C1/N1i−C1i bonds (Supporting Information, Table S2).

M06-2X/SVP optimized structures of the radical cation ($\mathbf{1}^{\bullet+}$) and dication ($\mathbf{1}^{2+}$) show appreciable difference in geometries, particularly in the central C_2 core and the C−C linkages of cAAC to the C_2 fragment (Supporting Information, Table S2). Under geometry optimizations, both $\mathbf{1}^{\bullet+}$ and $\mathbf{1}^{2+}$ undergo an analogous geometry change, resulting in a linear structure similar to that of **1**. There is, however, a very slight decrease in linearity of $\mathbf{1}^{2+}$ with respect to that of **1** (Supporting Information, Table S3). Stronger deviations in bond angles between the solid-state and gas-phase structures are not surprising (Supporting Information, Table S3). A similar observation was reported by Bestmann et al. in their model phosphonioboratoacetylene species and a possible explanation for such geometrical deviation is due to crystal packing effects.[21]

Calculations suggest that the structural deviation of $\mathbf{1}^{\bullet+}$ and $\mathbf{1}^{2+}$ with respect to **1** can be explained from the standpoint of lone-pair electron-density depletion on nitrogen atoms and accumulation at the central C_2 core. NBO analysis reveals that in $\mathbf{1}^{\bullet+}$ and $\mathbf{1}^{2+}$, lone pairs are missing on the nitrogen atoms unlike in **1**, indicating that electron density is delocalized to the neighboring C1 center, and N1−C1/N1i−C1i bonds become shorter in the cationic species (Supporting Information, Table S2). Similarly, an opposite trend is observed in C1−C21/C21i−C1i bonds, where we notice that the same bonds are elongated following the trend $\mathbf{1} > \mathbf{1}^{\bullet+} > \mathbf{1}^{2+}$. With subsequent oxidation of $\mathbf{1} \rightarrow \mathbf{1}^{\bullet+} \rightarrow \mathbf{1}^{2+}$, the electron density on the central C21−C21i bond becomes accumulated as is evidenced from the $\nabla^2\rho_b$ values (Supporting Information, Table S4), allowing the bond to strengthen (Supporting Information, Table S2). Furthermore, the decrease in ε_b (Supporting Information, Table S4) for the C1−C21/C21i−C1i and C21−C21i bonds as a consequence of oxidation implies that terminal and central double bonds are transformed to C−C single and triple bonds, respectively, both with higher cylindrical symmetry.[22] Based on our calculations, we consider that $\mathbf{1}^{\bullet+}$ and $\mathbf{1}^{2+}$ exhibit different resonance structures (Supporting Information, Schemes S2, S3). To evaluate the Lewis basicity of the C_4 species, we have calculated the energies for BH_3 association with **1** and $\mathbf{1}^{\bullet+}$ moieties. Formation of the BH_3 adduct $\mathbf{1}{\cdot}BH_3$ is more favorable ($\Delta G_{298} = 6.2$ kcal mol^{-1} for **1** vs. 20.5 kcal mol^{-1} for $\mathbf{1}^{\bullet+}$) than $\mathbf{1}^{\bullet+}{\cdot}BH_3$.[13a] The calculated ionization energies of **1**, $\mathbf{1}^{\bullet+}$, and $\mathbf{1}^{2+}$ are 5.1, 8.8, and 13.5 eV, respectively, which are comparable to those reported in $(cAAC)_2P_2$ species.[4] Compared to simple butatriene (C_4H_4) and other acetylenic compounds, the low first ionization energy of **1** can be attributed to a stable electronic ground state of $\mathbf{1}^{\bullet+}$, having extended delocalization of the positive charge (Supporting Information, Scheme S2).[16,23] The calculated hyperfine coupling constant of ^{14}N atoms in $\mathbf{1}^{\bullet+}$ is roughly 3.8 G (Supporting Information, Tables S5, S6), which is relatively close to the experimental value 5.3 G. The computed spin density values unfold the presence of roughly 60% of α-spin density on the C_4 unit and the rest residing on the N atoms (Supporting Information, Figure S11).

In summary, a novel synthesis of a 1,4-diamino derivative of C_4 cumulene **1** was developed by the reaction of cAAC, CBr_4, and K or Li. A systematic synthetic study showed that the primitive species $\mathbf{1}^{\bullet+}$ forms first, which further undergoes one-electron reduction to form the neutral species **1**. This was further confirmed by cyclic voltammogram, which also suggests the potential approach of a stable dication $\mathbf{1}^{2+}$. **1**, $\mathbf{1}^{\bullet+}$, and $\mathbf{1}^{2+}$ were synthesized and characterized by X-ray crystallography. The oxidation in the series of $\mathbf{1} \rightarrow \mathbf{1}^{\bullet+} \rightarrow \mathbf{1}^{2+}$ results in the increase of the electron density on the central C−C bond with the consequence that this bond is shortened and the terminal C−C bonds are elongated. EPR spectrum of $\mathbf{1}^{\bullet+}$ exhibits quintet hyperfine lines, which are originated from the coupling of the radical electron with two equivalent

nitrogen atoms. Both EPR and theoretical calculation indicate that the unpaired electron in $\mathbf{1}^{\bullet+}$ is mainly delocalized over the central C_4 backbone. Moreover, $\mathbf{1}^{\bullet+}TfO^-$ is stable in air, despite it having a radical character.

Received: December 18, 2013
Published online: March 12, 2014

Keywords: cumulenes · cyclic alkyl(amino) carbenes · dications · radical ions · theoretical calculations

[1] a) Y. Wang, Y. Xie, P. Wei, R. B. King, H. F. Schäfer III, P. von R. Schleyer, G. H. Robinson, *Science* **2008**, *321*, 1069 – 1071; b) C. D. Martin, M. Soleilhavoup, G. Bertrand, *Chem. Sci.* **2013**, *4*, 3020 – 3030; c) Y. Wang, G. H. Robinson, *Chem. Commun.* **2009**, 5201 – 5213.

[2] a) V. Lavallo, Y. Canac, C. Präsang, B. Donnadieu, G. Bertrand, *Angew. Chem.* **2005**, *117*, 5851 – 5855; *Angew. Chem. Int. Ed.* **2005**, *44*, 5705 – 5709; b) D. Martin, M. Melaimi, M. Soleilhavoup, G. Bertrand, *Organometallics* **2011**, *30*, 5304 – 5313; c) O. Back, M. Henry-Ellinger, C. D. Martin, D. Martin, G. Bertrand, *Angew. Chem.* **2013**, *125*, 3011 – 3015; *Angew. Chem. Int. Ed.* **2013**, *52*, 2939 – 2943; d) D. Martin, M. Soleilhavoup, G. Bertrand, *Chem. Sci.* **2011**, *2*, 389 – 399.

[3] R. Kinjo, B. Donnadieu, G. Bertrand, *Angew. Chem.* **2010**, *122*, 6066 – 6069; *Angew. Chem. Int. Ed.* **2010**, *49*, 5930 – 5933.

[4] O. Back, B. Donnadieu, P. Parameswaran, G. Frenking, G. Bertrand, *Nat. Chem.* **2010**, *2*, 369 – 373.

[5] O. Back, M. A. Celik, G. Frenking, M. Melaimi, B. Donnadieu, G. Bertrand, *J. Am. Chem. Soc.* **2010**, *132*, 10262 – 10263.

[6] R. Kinjo, B. Donnadieu, M. A. Celik, G. Frenking, G. Bertrand, *Science* **2011**, *333*, 610 – 613.

[7] V. Lavallo, Y. Canac, B. Donnadieu, W. W. Schoeller, G. Bertrand, *Angew. Chem.* **2006**, *118*, 3568 – 3571; *Angew. Chem. Int. Ed.* **2006**, *45*, 3488 – 3491.

[8] a) K. C. Mondal, H. W. Roesky, M. C. Schwarzer, G. Frenking, B. Niepötter, H. Wolf, R. Herbst-Irmer, D. Stalke, *Angew. Chem.* **2013**, *125*, 3036 – 3040; *Angew. Chem. Int. Ed.* **2013**, *52*, 2963 – 2967; b) K. C. Mondal, P. P. Samuel, M. Tretiakov, A. P. Singh, H. W. Roesky, A. C. Stückl, B. Niepötter, E. Carl, H. Wolf, R. Herbst-Irmer, D. Stalke, *Inorg. Chem.* **2013**, *52*, 4736 – 4743.

[9] Y. Li, K. C. Mondal, H. W. Roesky, H. Zhu, P. Stollberg, R. Herbst-Irmer, D. Stalke, D. M. Andrada, *J. Am. Chem. Soc.* **2013**, *135*, 12422 – 12428.

[10] K. C. Mondal, H. W. Roesky, B. Dittrich, N. Holzmann, M. Hermann, G. Frenking, A. Meents, *J. Am. Chem. Soc.* **2013**, *135*, 15990 – 15993.

[11] a) C. A. Dyker, V. Lavallo, B. Donnadieu, G. Bertrand, *Angew. Chem.* **2008**, *120*, 3250 – 3253; *Angew. Chem. Int. Ed.* **2008**, *47*, 3206 – 3209; b) R. Tonner, G. Frenking, *Angew. Chem.* **2007**, *119*, 8850 – 8853; *Angew. Chem. Int. Ed.* **2007**, *46*, 8695 – 8698; c) M. Alcarazo, C. W. Lehmann, A. Anoop, W. Thiel, A. Füstner, *Nat. Chem.* **2009**, *1*, 295 – 301; d) A. Fürstner, M. Alcarazo, R. Goddard, C. W. Lehmann, *Angew. Chem.* **2008**, *120*, 3254 – 3258; *Angew. Chem. Int. Ed.* **2008**, *47*, 3210 – 3214.

[12] A. Sidiropoulos, C. Jones, A. Stasch, S. Klein, G. Frenking, *Angew. Chem.* **2009**, *121*, 9881 – 9884; *Angew. Chem. Int. Ed.* **2009**, *48*, 9701 – 9704.

[13] a) J. L. Dutton, D. J. D. Wilson, *Angew. Chem.* **2012**, *124*, 1506 – 1509; *Angew. Chem. Int. Ed.* **2012**, *51*, 1477 – 1480; b) R. I. Kaiser, *Chem. Rev.* **2002**, *102*, 1309 – 1358; c) W. Weltner, R. J. Van Zee, *Chem. Rev.* **1989**, *89*, 1713 – 1747.

[14] a) L. Leroyer, V. Maraval, R. Chauvin, *Chem. Rev.* **2012**, *112*, 1310 – 1343; b) D. Cremer, E. Kraka, H. Joo, J. A. Stearns, T. S. Zwier, *Phys. Chem. Chem. Phys.* **2006**, *8*, 5304 – 5316 and references therein; c) R. Chauvin, *Tetrahedron Lett.* **1995**, *36*, 397 – 400.

[15] a) P. F. Schwab, M. D. Levin, J. Michl, *Chem. Rev.* **1999**, *99*, 1863 – 1934; b) F. Paul, W. E. Meyer, L. Toupet, H. Jiao, J. A. Gladysz, C. Lapinte, *J. Am. Chem. Soc.* **2000**, *122*, 9405 – 9414.

[16] W. Kaim, H. Bock, *J. Organomet. Chem.* **1979**, *164*, 281 – 293.

[17] The reason for the formation of the red color is still not clear. It is perhaps due to the generation of CBr_3 or Br radicals in the presence of cAAC. See: Q. Kong, M. Wulff, J. H. Lee, S. Bratos, H. Ihee, *J. Am. Chem. Soc.* **2007**, *129*, 13584 – 13591 and the references therein.

[18] The calculated molar ratio of C_4^+ and TfO^- anion is 1:1 in the real structure of $\mathbf{1}^{\bullet+}TfO^-\cdot THF\cdot H_2O$.

[19] The calculated molar ratio of C_4^+ and $H(NO_3)_2^-$ anion is 1:2 in the real structure of $\mathbf{1}^{2+}[H(NO_3)_2^-]_2$.

[20] Gaussian 09 (Revision C.01), M. J. Frisch, et al. Gaussian, Inc., Wallingford CT, **2009**. For full references, see the Supporting Information.

[21] a) H. J. Bestmann, H. Behl, M. Bremer, *Angew. Chem.* **1989**, *101*, 1303 – 1304; *Angew. Chem. Int. Ed. Engl.* **1989**, *28*, 1219 – 1221; b) G. Trinquier, J. P. Malrien, *J. Am. Chem. Soc.* **1987**, *109*, 5303 – 5315.

[22] *The Quantum Theory of Atoms in Molecules* (Eds.: C. F. Matta, R. J. Boyd), Wiley-VCH, Weinheim, **2007**.

[23] F. Brogli, E. Heilbronner, E. Kloster-Jensen, A. Schmelzer, A. S. Manocha, J. A. Pople, L. Radom, *Chem. Phys.* **1974**, *4*, 107 – 119.